A user-defined Folgar-Tucker-based fiber orientation material model for compression molding of fiber/polymer-compounds

Dominic Schommer[1], Miro Duhovic[1], David May[1], Joachim Hausmann[1], Heiko Andrä[2], Konrad Steiner[2]

[1] Leibniz-Institut für Verbundwerkstoffe GmbH, Rheinland-Pfälzische Technische Universität Kaiserslautern-Landau, Germany
[2] Fraunhofer ITWM, Kaiserslautern, Germany

Abstract. LS-DYNA® provides an ever-increasing portfolio of material models covering a wide range of material behavior for solving multi-physics problems. The software also provides users the opportunity to implement their own user-defined material models via FORTRAN code, to describe the behavior of very specific materials. In this work, a user-defined material model has been developed to describe the compression molding behavior of sheet molding compounds (SMCs). A SMC is a composite material based on a thermoset resin reinforced by chopped long fibers. During the compression molding of SMCs, very complex material behavior involving elastic compaction and plastic flow (depending on material composition) occurs, which is dependent on the local fiber orientation, temperature and strain rate. One way to describe the processing behavior of SMC materials as simply as possible is using a building block approach. Following the identification of the most relevant material effects, individual building blocks are created containing the respective mathematical solutions (e.g. compaction and plastic flow behavior). Each building block is coupled with its neighboring block via its input and output parameters. In this way, complex composite material processing behavior can be simulated using individual building blocks representing individual mathematical models, which can be added or removed as required. Since no material model in the current LS-DYNA solver considers the evolution of fiber orientation (FO) during flow processing of short- or long-fiber reinforced composites, the integration of such an individual building block is presented here. Specifically, the influence of FO on a non-linear elastic piecewise plastic material model is considered. In this example, a FO model based on the Folgar-Tucker equation is implemented and applied to Arbitrary Lagrangian Eulerian (ALE) elements. To determine the position of the FO building block within the complete SMC material model structure, the required input information to the model and the possible output information from one building block to another is identified. Subsequently, a subroutine containing the corresponding FO mathematical model is written and called within the material function. As a conclusion, it is shown how the implemented FO model behaves during compression molding simulations and how the resulting FO information can be evaluated at the post-processing stage using LS-PrePost® and Python.

1 Introduction

Fiber/Polymer compound materials represent a popular category of lightweight composite materials consisting of discontinuous fiber reinforcements combined with a thermoset or thermoplastic resin system. This group of materials allows the reduction of component weight and an increase in mechanical properties over neat plastic parts by using short or long fiber reinforcements. The so-called Sheet Molding Compound (SMC) is a thermoset-based subgroup, which can be processed by simple compression molding with low cycle times and process costs [1]. SMCs are characterized by high flowability and therefore offer a high degree of design freedom for thin-walled structural and non-structural components with rib structures and wall thickness variations [2]. When investigating and modeling the compression molding process in detail, one encounters very complex material behavior, which is due to the diverse composition possibilities within the SMC material group. This diversity is somewhat caused by the use of SMC materials in a wide range of applications, for example insulating enclosures (battery boxes) in the electrical sector, Class-A surface quality or flame-retardant behavior. In general, SMCs are based on a thermoset resin (in most cases an unsaturated polyester, vinyl ester or epoxy resin system), which contains application specific mineral or bio-based fillers and additives [3], [4]. The fiber reinforcement usually consists of up to 30% by weight chopped glass fibers or, for even better mechanical properties, up to 50% by weight carbon fibers. To guarantee the required mechanical properties, the typical fiber length is 25 to 50 mm [1], [5]. The behavior of SMC materials during compression molding includes a few characteristic properties, which is briefly discussed here.

The first important aspect is the mechanical behavior. Due to the pressure applied during compression molding, SMCs show a characteristic initial compaction phase of the fiber reinforcement structure at the first stages of compression without any in-plane flow. Here the fibers are compacted and gases (e.g. air and styrol) are pressed out of the material. In the second phase of compression, a compressible plastic flow sets in as soon as the initial compaction phase has finished. This mechanical behavior results in a characteristic stress-strain behavior that depends on the fiber properties, fiber content, fiber distribution and fiber orientation in all three spatial directions as well as on the strain-rate dependent viscosity of the thermoset resin [6]. The second important aspect is the flow front behavior during the compressible plastic flow phase of compression molding. Here, an in-plane anisotropic flow front development can be observed, which is dependent on the local fiber orientation. In the thickness direction, in the optimal case, a plug flow dominates the flow behavior. In the contact areas between tool and SMC material, shear flow overlaps the plug flow caused by contact interactions (e.g. wall friction) [7], [8]. In reality, the higher temperature of the hot tooling causes a decrease in the viscosity of the resin and so a faster movement of the outer SMC layers [9]. A third important aspect is the chemical curing reaction of the thermoset resin, which is activated at elevated temperatures. Since the flowability decreases with curing, an optimal filling result during compression molding can only be achieved, if the mold has been completely closed before the curing reaction starts. Therefore, the curing is a minor aspect of process simulation but highly important for subsequent warpage simulations [2], [6], [10].
Taking into account the aspects discussed above, it can be seen that the overall behavior of SMC during compression molding depends on a complex combination of mechanical, thermal and chemical properties. The goal of this paper is to show LS-DYNA® users a concept for considering all these aspects combined in one user-defined material model. At the time of writing, there is currently no material model available in LS-DYNA® that considers a macroscopic model for fiber orientation evolution during flow processes, (even in the latest draft version of the Keyword User's Manual Volume II Material Models, master@48596c3b8 (07/12/23)) [11]. This paper therefore demonstrates in detail the inclusion of a Folgar-Tucker based fiber orientation model and post-processing of the fiber orientation information allowing comparisons of flow front development and fiber orientation with real experiments.

2 Set-up of User-defined material model

To gain access to the implementation possibilities of your own user-defined material model, you have to download the so-called "object version" of LS-DYNA®. The "object version" is a zipped package, which contains a "usermat" directory, consisting of precompiled "static object" libraries, FORTRAN source code files, "include" files and a Makefile. Via the FORTRAN source code files the user is able to directly integrate his own models into the existing FORTRAN code. Users not only have the possibility to create their own material models and thermal models, but they can also program their own equation of state (EOS), element formulations for volume and shell elements, airbag sensors, friction and conductivity models, as well as solution and interface controls [12]. However, this paper will focus on the creation of material models. Compiling the package creates an executable solver file that can be used to run a simulation. When compiling the unchanged package, the new solver file is identical to the regular LS-DYNA® solver of the corresponding software version.
The user obtains access to the user-defined material models via the keyword ***MAT_USER_DEFINED_MATERIAL_MODELS**, where the material numbers ***MAT_041-050** are assigned to allow reference to these material models. Therefore, it is possible to use up to 10 different user-defined material models within one simulation. The assigned material number corresponds also to the used subroutine number in the FORTRAN source code.

The user-defined material model for the representation of the flow behavior of SMC during compression molding is built-up from the following two considerations.

1. The material model shall include all necessary properties of a SMC semi-finished product to represent the flow characteristics efficiently and accurately.
2. A research basis is created, whereby each significant property is represented by individual mathematical descriptions and all properties are coupled to represent the complex material behavior. Later access for the further development of the individual models should be made possible.

The result of these considerations is a classical building block approach, where individual building blocks adopt a single property of the material and communicate with one another by passing input and output parameters to neighboring building blocks. Fig.1: shows an example building block constellation for the set-up of an SMC material model. The thermal and chemical descriptions are an optional inclusion into

the model as users have the possibility to define their own or use the available thermal and curing models in LS-DYNA®.

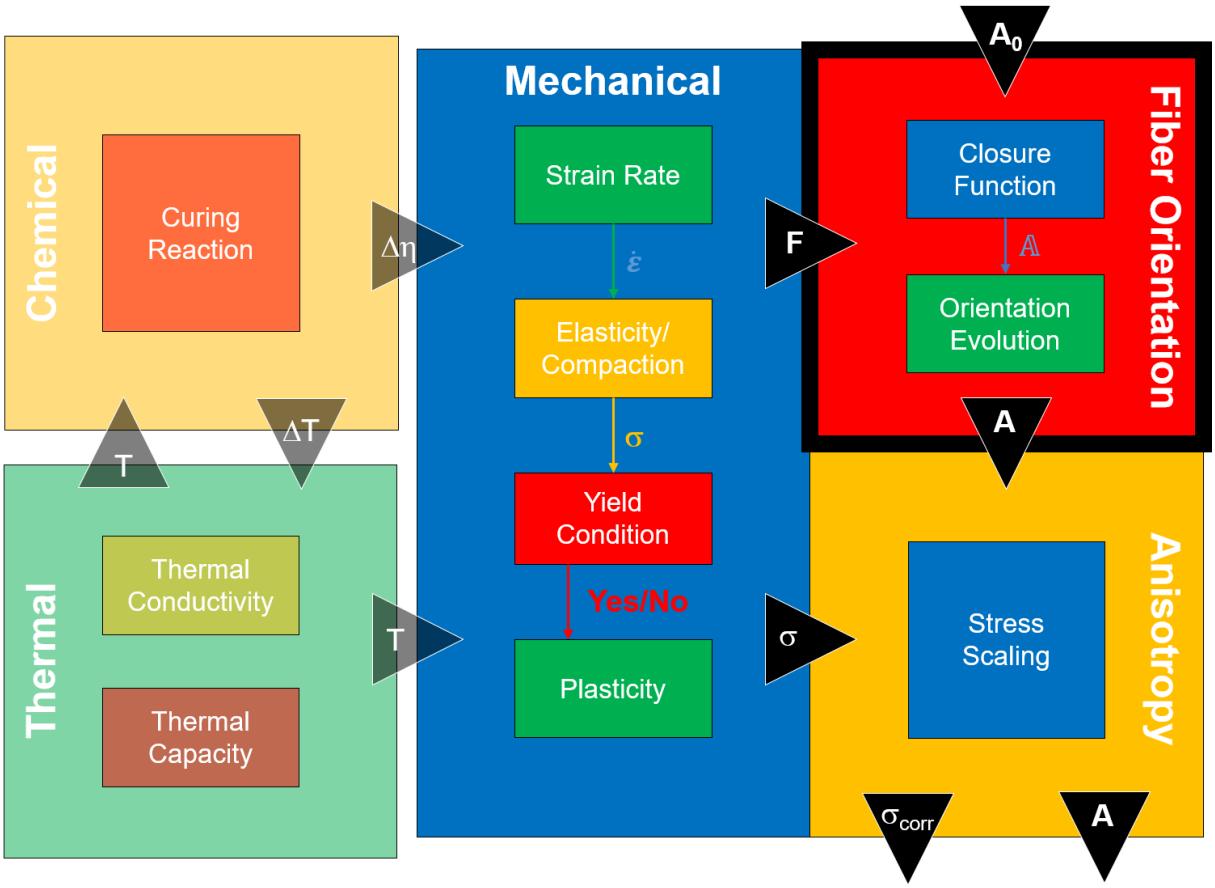

Fig.1: Example constellation of building block approach for SMC material (symbols explained in section 3).

By using this approach, building blocks can be integrated into the model in two different modes. In the current existing version of the material model, only one solution for each building block is realized. Therefore, it makes sense to include the building blocks in a single usermat subroutine as a serial sequence. With the aforementioned second consideration in mind, in further developments, a separate subroutine should be written for each block, which is called in the main subroutine. This improves the interchangeability of individual aspects and makes the model more flexible and efficient.

Within the scope of this paper, it is not possible to describe each individual building block. So it was decided to concentrate on the description of implementation and communication of one single building block that represents a macroscopic description of the fiber orientation evolution during the compression molding process (highlighted by a black frame in Fig.1:).

3 Description of fiber orientation

The modeling of the fiber orientation evolution can be achieved on a microscopic or on a macroscopic level. Looking at the fibers at the microscopic level allows a detailed analysis of the physical behavior of the individual fibers, as well as the interaction of the fibers with each other and the fibers with the surrounding matrix and any fillers present. Hayashi et al. [13]–[15] showed examples for a microscopic modeling approach for compression molding of long fiber reinforced composite materials in previous LS-DYNA® conferences. Other groups have also made progress in this direction terming the method direct fiber simulation (DFS) [16] or direct bundle simulations [17] and have further developed the methodologies in this direction. In general, however, these models require a separate geometric model for the resin material and the fiber reinforcement structure. For this reason, these methods are usually very resource-intensive and are therefore not suitable in many cases for viewing models at the component level. In this paper, a macroscopic modeling approach is used to include the fiber orientation directly within the material model. Unfortunately, this is a simplification, as it does not take into account

all the physical effects due to the length of the fibers. Nevertheless, for a first realization it is possible to rely on fiber orientation models already established in other simulation software, mostly for modelling short or long fiber flow processes. In general, these models are based on the approach of Folgar and Tucker [18]. The Folgar-Tucker equation (1) predicts the continuous evolution of the 2nd order fiber orientation tensor $\boldsymbol{A}$ considering a probability distribution function Ψ [19].

$$\frac{D\boldsymbol{A}}{Dt} = (\boldsymbol{W}\cdot\boldsymbol{A} - \boldsymbol{A}\cdot\boldsymbol{W}) + \xi(\boldsymbol{D}\cdot\boldsymbol{A} + \boldsymbol{A}\cdot\boldsymbol{D} - 2\mathbb{A}\!:\!\boldsymbol{D}) + 2C_i\dot{\gamma}(\boldsymbol{I} - 3\boldsymbol{A}) \tag{1}$$

ξ is the underlying geometry factor, whose value is determined by the shape of the fiber considered. The vorticity tensor $\boldsymbol{W}$ (2) and the deformation tensor $\boldsymbol{D}$ (3) depend on the velocity gradient $\boldsymbol{L}$. When using user-defined materials in LS-DYNA®, the velocity gradient is unfortunately not a directly available parameter, but can be calculated via the deformation gradient $\boldsymbol{F}$ (4). By activation of the flag "IHYPER" in the material card for user defined materials, access to the deformation gradient can be obtained.

$$\boldsymbol{W} = \frac{1}{2}(\boldsymbol{L} - \boldsymbol{L}^T) \tag{2}$$

$$\boldsymbol{D} = \frac{1}{2}(\boldsymbol{L} + \boldsymbol{L}^T) \tag{3}$$

$$\boldsymbol{L} = \dot{\boldsymbol{F}}\boldsymbol{F}^{\boldsymbol{T}} \tag{4}$$

The components of the 2nd order fiber orientation tensor $\boldsymbol{A}$ correspond to:

$$\boldsymbol{A_{ij}} = \langle p_i p_j \rangle \triangleq \oint \Psi(\boldsymbol{p}) p_i p_j d\boldsymbol{p} \tag{5}$$

And the components of the 4th order fiber orientation tensor $\mathbb{A}$:

$$\mathbb{A}_{\boldsymbol{ijkl}} = \langle \boldsymbol{p_i p_j p_k p_l} \rangle \triangleq \oint \Psi(\boldsymbol{p}) \boldsymbol{p_i p_j p_k p_l} \boldsymbol{dp} \tag{6}$$

The brackets $\langle\ \ \rangle$ stand for the average of all possible spatial directions $\boldsymbol{p}$ in which the orientation vector $\boldsymbol{p}$ of the fiber can be oriented, weighted by the function $\Psi(\boldsymbol{p})$. The diffusion coefficient C_i describes the interaction between fibers. C_i is an empirical value that usually must be determined experimentally. $\dot{\gamma}$ is the magnitude of the strain rate tensor and $\boldsymbol{I}$ represents the 2nd order unit tensor.
The typical visualization of the fiber orientation tensor is given by an ellipsoid (Fig.2:). The products of the eigenvalues λ_i and the eigenvectors $\vec{e_i}$ define the main orientation directions of the fiber orientation distribution for the considered volume. The outer surface of the ellipsoid describes the probabilities of fibers oriented in all spatial directions. In the simulation, the considered volume is usually defined as one element of the finite element mesh.

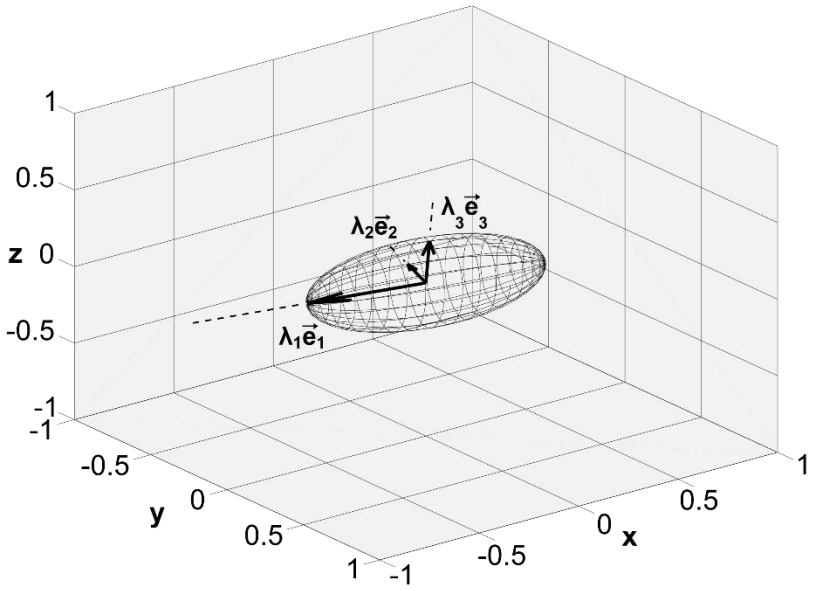

*Fig.2: Representation of the fiber orientation tensor **A** as an ellipsoid.*

On closer inspection, the Folgar-Tucker equation shows some weaknesses in predicting fiber orientation. For example, the model is known for over predicting the rotary diffusion of the fiber movement. In addition, the model tends to work well for short fiber reinforcement (fiber length up to 2 mm), but is not always accurate for long fiber cases (fiber lengths of 10 – 12 mm) [20]. For these reasons, evolution of the original Folgar-Tucker equation has occurred over the years with the aim to correct some of its shortcomings. Fig.3: shows an overview of this development without claiming to be complete. In this paper, we do not refer to the individual models, but only to the variant implemented in the user-defined material model.

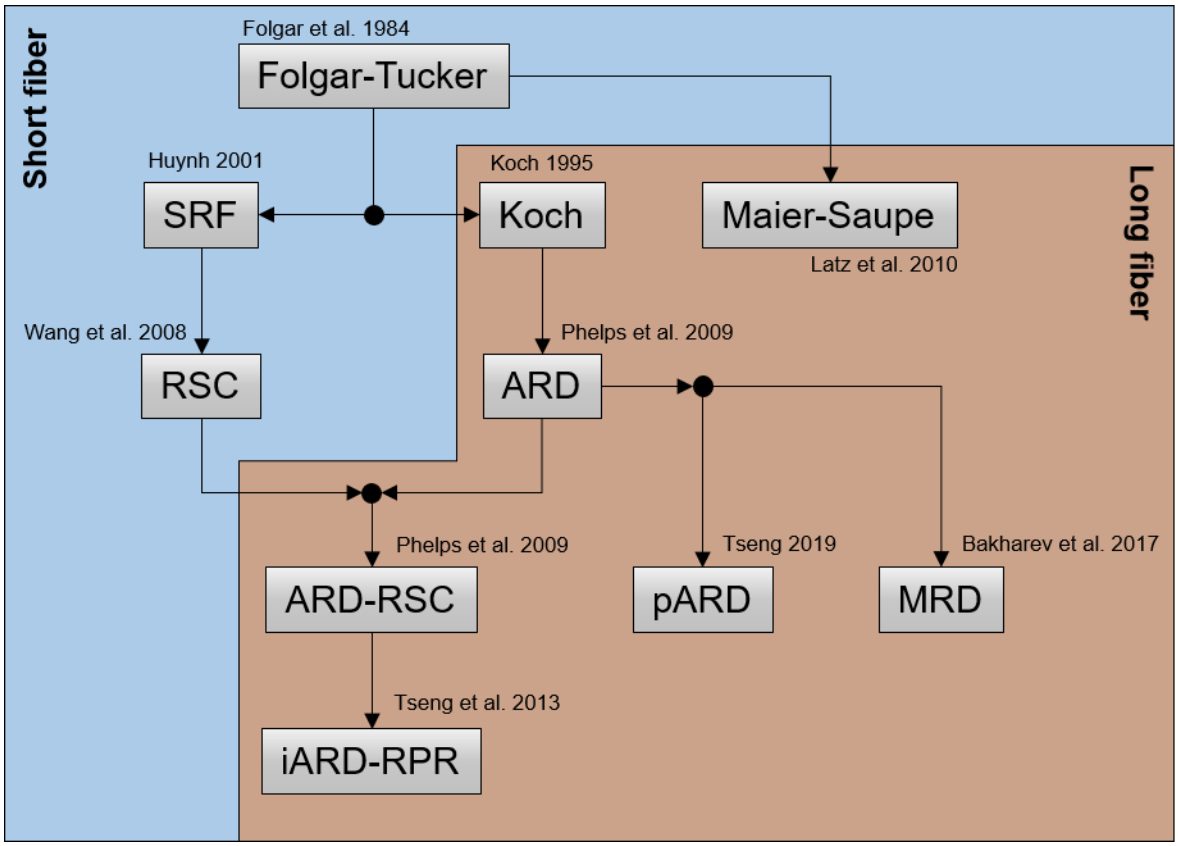

Fig.3: Overview of macroscopic fiber orientation models based on the Folgar-Tucker equation [18], [21]–[28].

In this work, a modified Folgar-Tucker model with connected Maier-Saupe term is implemented. It is a model, in which the fiber orientation and the motion of the surrounding flow are fully coupled. For this purpose, the Folgar-Tucker model is modified by introducing a nematic potential in the Maier-Saupe form (7). [25]

$$\frac{D\boldsymbol{A}}{Dt} = \boldsymbol{M}\boldsymbol{A} + \boldsymbol{A}\boldsymbol{M}^T - 2\mathbb{A}:\boldsymbol{M} - 6C_i\dot{\gamma}\left(\boldsymbol{A} - \frac{1}{3}\boldsymbol{I}\right) \tag{7}$$

With Maier-Saupe term (8):

$$\boldsymbol{M} = \xi\boldsymbol{D} + \boldsymbol{W} + \dot{\gamma}U_0\boldsymbol{A} \tag{8}$$

In our case, a long fiber reinforcement is considered, where the length of the fiber is much larger than the diameter, so a geometry factor $\xi = 1$ is obtained. It is assumed that the interaction between the fibers is mainly determined by the velocity gradient. Therefore, the proportionality factor of the nematic potential is expressed by $\dot{\gamma}U_0$ [25]. For this material model, U_0 is an experimental fitted parameter. The absolute value of the strain rate tensor $\dot{\gamma}$ (9) is determined via the deformation tensor $\boldsymbol{D}$ (3).

$$\dot{\gamma} = \sqrt{\frac{1}{2}\boldsymbol{D}:\boldsymbol{D}} \tag{9}$$

A number of closure functions are available for determining the 4th order orientation tensor $\mathbb{A}$. For the calculation of fiber orientation, the functions Invariant Based Optimal Fitting (IBOF), Bingham or Hybrid

are often used. For this user-defined material model, we were looking for a stable and simple to implement closure function and decided for a simple quadratic function (10).

$$\mathbb{A} = \boldsymbol{A} \otimes \boldsymbol{A} \tag{10}$$

Now that the fiber orientation model has been specified, the input and output parameters of the model result. This also fixes the position of the fiber orientation block in the model. Input parameter here does not mean the material parameters given by the material card. Instead, it means the input parameter from the solver calculation. In fact, there are just two necessary parameters. One is the initial 2nd order fiber orientation tensor $\boldsymbol{A_0}$, that is the resulting $\boldsymbol{A}$ from the previous time-step or in case of the first time-step, the initial fiber orientation given by the material card. The second parameter is the deformation gradient $\boldsymbol{F}$, necessary to calculate the velocity gradient $\boldsymbol{L}$. The deformation gradient $\boldsymbol{F}$ is a result of the mechanical calculation of the previous time-step. This means the fiber orientation calculation is just based on information from the previous time-step and is therefore uncoupled from the mechanical calculation of the current time-step. Therefore, it makes no difference, if we place it before or after the mechanical calculation. The result is the updated 2nd order fiber orientation tensor $\boldsymbol{A}$, that is used for the calculation of the anisotropy of the mechanical behavior. The output of the six components of the symmetric tensor is handled by history variables whose number is defined in the material card and can be visualized in LS-PrePost®. Fig.4: shows the graphical visualization of the three main components of the 2nd order fiber orientation tensor during the compression molding of an automotive rear wing demonstrator component.

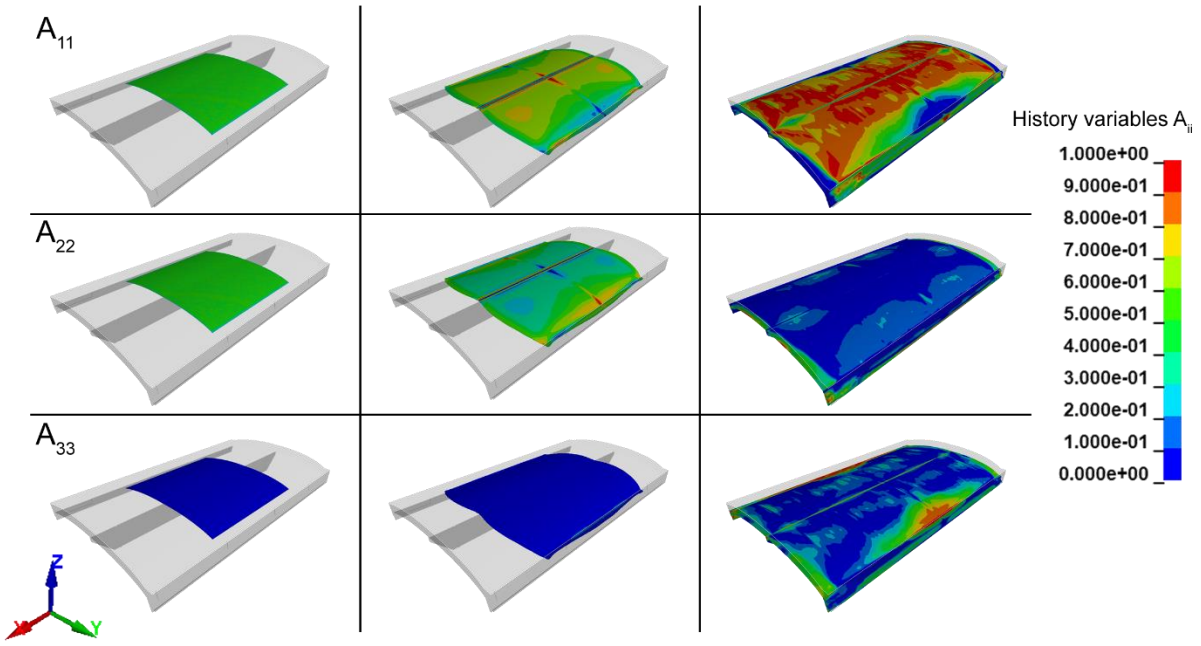

Fig.4: Output of user-defined history variables for fiber orientation tensor during a compression molding simulation. The initial fiber orientation is defined as in-plane isotropic with $A_{11} = 0.5$, $A_{22} = 0.5$ and $A_{33} = 0$.

4 Post-Processing of fiber orientation information

One of the main goals in post-processing the fiber orientation information in this work has been to enable direct comparisons with experimental measurements. As an example, consider the images presented in Fig.5:, which show experimental (left), and simulation (right) generated images of the surface fiber orientation for a carbon fiber reinforced SMC material (C-SMC) test specimen. The experimental technique used here, which was first developed by the Fraunhofer Institute for Integrated Circuits (IIS), uses a method to measure surface fiber orientation in carbon fiber reinforced polymers (CFRP) by analyzing the polarization direction of light reflected from the CFRP test object [29], [30]. When non-polarized light hits the carbon fiber, reflected light is polarized based on the direction of the fiber. The result of the measurement is the pixel-wise fiber orientation angle within the image plane. For a simple explanation, this paper uses the basic geometry from a press rheometry SMC material characterization

test. Further information about the polarization imaging technique for experimental fiber orientation measurement can also be found in [31].
The original shape of the test specimen is a 100x100 mm square. When performing the press rheometry test, the tool gap closes and the SMC material flows in-plane under pressure and forms a more or less circular shape. The top images shows the specimen at a tool gap of 8 mm. At this tool position only compression and no plastic flow has taken place and the shown fiber orientation angles can be seen as the initial orientation. The bottom images show the specimen at a tool gap of 3 mm. This thickness represents a typical wall thickness of SMC components. The coloring shows a clear reorientation of the fibers in direction of the material flow. This is also consistent with the assumptions of the Folgar-Tucker equation. The original data from the polarization imaging are grey scale images, where the grey value represents the fiber orientation angle. For better visualization, the images are colored with a continuous color map that can be made equivalent for both the experimental images and the simulation plots.

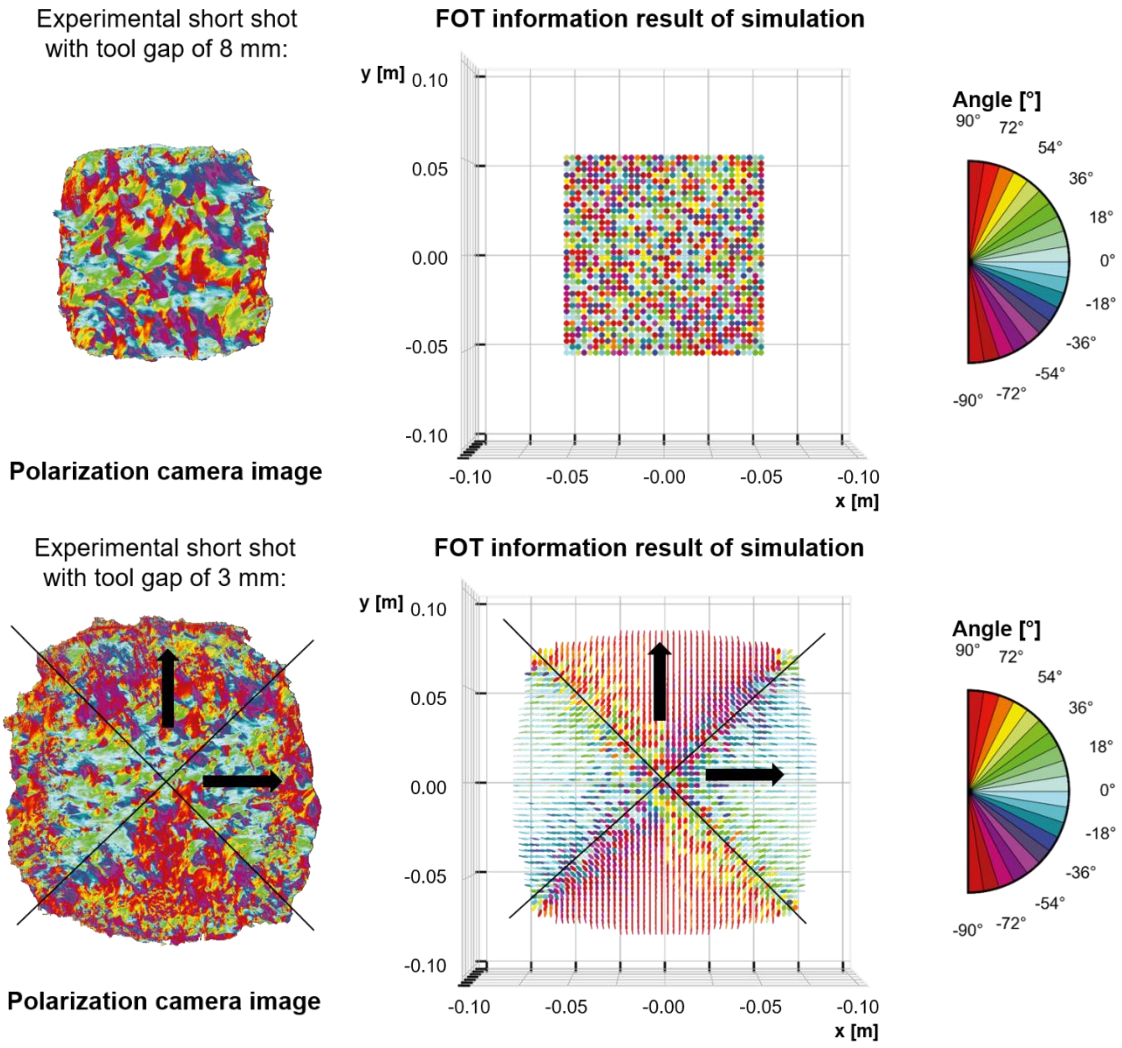

Fig.5: Comparison of experimental polarization imaging fiber orientation measurement (left) and simulation of a press rheometry test specimen (right).

To compare the simulation results with experimental measurements of the fiber orientation using a polarization camera, it is necessary to determine the fiber orientation angle in a predefined plane. Currently, only information for the fiber orientation tensor in three-dimensional space is available from the FEM result stored in the history variables 1 to 6. This information needs to be converted to a fiber orientation angle. This conversion is carried out by using a Python script. The first question is how to extract the history variable information and provide access to this data within the python script. One option is to use the free qd python library [32] to provide direct access to the d3plot data. Unfortunately, this python library does not support the ALE method used in this work. Therefore, the alternative option is to use the LS-PrePost® output options directly. The required history variable data is available via **`POST -> History -> Element`** and can be read out as a graph over time for each selected element.

The data from the chart can now be exported as a txt or csv file. It is recommended to use the MSoft CSV(Single X-Axis) format to obtain the formatting shown in Table 1:. Here, the time is the x-axis in the first column and applies to all other columns. This is followed by a block of columns of the first history variable (corresponding to component $\boldsymbol{A}_{11}$ of the fiber orientation tensor) for each selected element. This block is repeated for each desired history variable.

Time	*Hist-Var. #1-El. ID*	*Hist-Var. #2-El. ID*	*Hist-Var. #3-El. ID*	*Hist-Var. #4-El. ID*	*Hist-Var. #5-El. ID*	*Hist-Var. #6-El. ID*

Table 1: Formatting the output of the fiber orientation when using the MSoft CSV(Single X-Axis) format.

This procedure is very time consuming. Therefore, it is recommended just to visualize certain regions of interest (ROI) or to edit the complete component over several selected steps.
The visualization of the fiber orientation tensor is a simple drawing of the ellipsoid defined by the eigenvector and eigenvalue of the tensor and the element center coordinates and is not considered any further here. Of greater interest is the determination of the 2D fiber orientation angles when viewing elements of the part across various section planes. First, the main fiber directions in the defined plane are searched. In our example, the polarization camera is looking on the top surface of the specimen. Therefore, in the simulation the defined plane is the principal xy-plane. To determine the main fiber direction, the principal axis $V_i = \lambda_i \vec{e}_i$ of the fiber orientation tensor are projected onto the xy-plane and the resulting main fiber angle ϕ is determined using the components (x, y, z) of the projected vector. In formulae (11) and (12), the example of a projection onto the xy-plane is shown. Here $\vec{u}$ and $\vec{v}$ are two unit vectors spanning the plane.

$$\vec{V}_{Proj,i} = (\vec{V}_i \cdot \vec{u})\,\vec{u} + (\vec{V}_i \cdot \vec{v})\,\vec{v} \tag{11}$$

with $i = 1,2,3$ and $\vec{u} = \begin{pmatrix} 1 \\ 0 \\ 0 \end{pmatrix}$ and $\vec{v} = \begin{pmatrix} 0 \\ 1 \\ 0 \end{pmatrix}$

$$\phi = tan^{-1}\left(\frac{\vec{V}_{proj,1} \cdot \vec{v}}{\vec{V}_{proj,1} \cdot \vec{u}}\right) \tag{12}$$

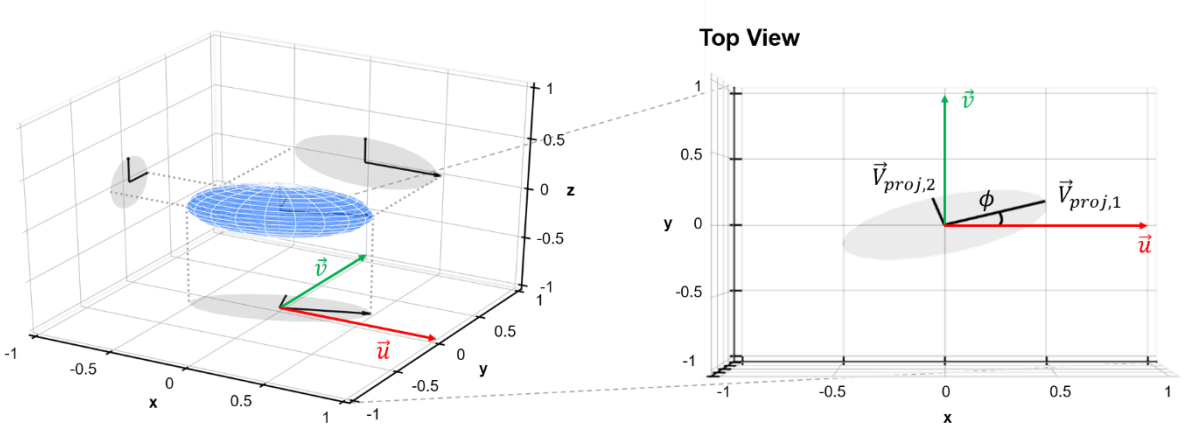

Fig.6: Projection of the 2nd order fiber orientation tensor onto the three principal planes.

However, since the ellipsoid indicates the probability of the main fiber angle ϕ occurring, this must also be taken into account when specifying the angle. As an example, for an in-plane isotropic fiber distribution over the entire plane the fibers are statistically uniformly oriented at all fiber angles. The angle ϕ, however, would always result in 0°, what wrongly indicates a unidirectional material. Accordingly, the probability distribution of a certain fiber orientation angle within an element is calculated via a weighted random selection in the python script.
The probability κ_1 that the angle ϕ occurs corresponds to the Euclidean norm of the projected vector (13). The probability κ_2 that $\phi \pm 90°$ occurs corresponds to the difference of the sum of the norms of all three projected vectors (one always corresponds to the zero vector) and the norm of the vector in the main fiber direction (14).

$$\kappa_1 = \left\|\vec{V}_{proj,1}\right\|_2 \tag{13}$$

$$\kappa_2 = \left(\sum_{i=1}^{3}\left\|\vec{V}_{proj,i}\right\|_2\right) - \left\|\vec{V}_{proj,1}\right\|_2 \tag{14}$$

A linear interpolation is used to calculate the probabilities for all angles in the range [ϕ - Limit, ϕ + Limit]. It should be noted that the range of all theoretically possible angles is [-90°, 90°]. The two ranges form an intersection. The probability of all angles outside this intersection is zero. The parameter Limit is necessary to restrict the space of possible angles. For example, for an isotropic material, all angles in [-90°, 90°] could be possible, so Limit = 90°. In a unidirectional material just the main fiber orientation angle is a possible solution, so Limit = 0°. In the general case, Limit can be obtained dependent of the probability κ_1 (13) by a linear interpolation (Fig.7:) between the maximum probability κ_{max} (15) and the minimum probability κ_{min} (16).

$$\kappa_{min} = 0.5\sum_{i=1}^{3}\left\|\vec{V}_{proj,i}\right\|_2 \tag{15}$$

$$\kappa_{max} = \sum_{i=1}^{3}\left\|\vec{V}_{proj,i}\right\|_2 \tag{16}$$

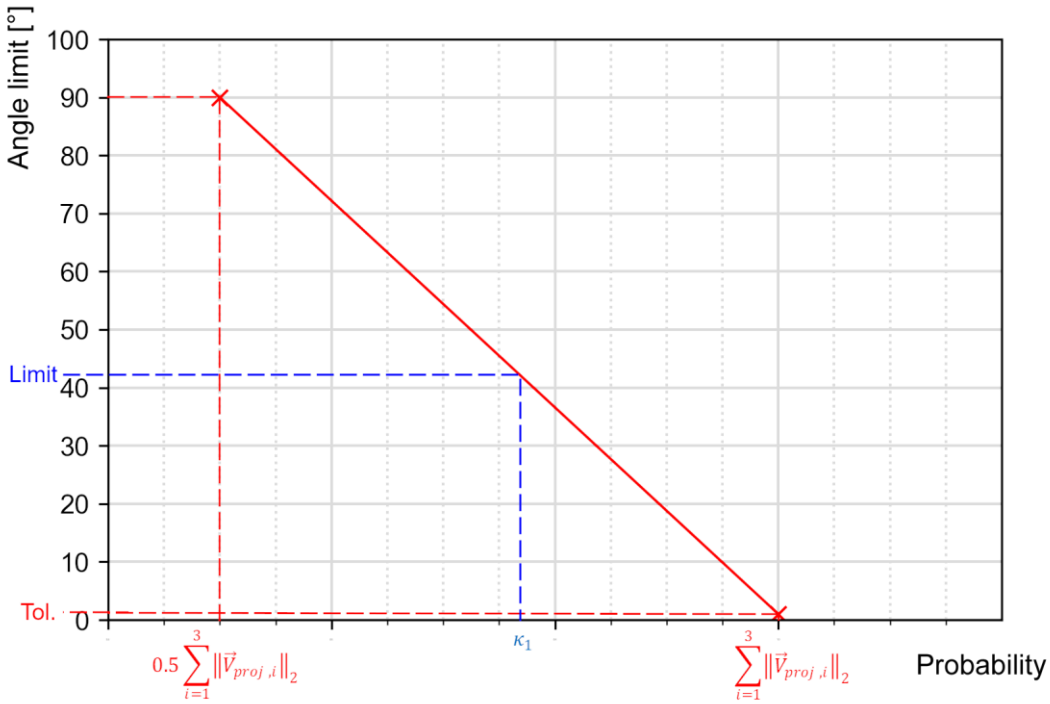

Fig.7: Linear interpolation of the angle limits for determination of 2D section plane fiber orientation angle.

The python script goes through this procedure and creates a visualization of the 2nd order fiber orientation angles for each element in the ROI and colors it for the corresponding fiber orientation angle. Fig.5: on the right side shows the simulation results for the press rheometry specimen. The initial state is defined as an in-plane isotropic fiber distribution with $A_{11} = 0.5$, $A_{22} = 0.5$ and $A_{33} = 0$. All ellipsoids have a circular shape and are initially randomly colored within the range of all possible fiber orientation angles from -90° to 90°. In comparison with the experimental measurement on the left side, one disadvantage of the macroscopic fiber orientation model can be seen here. Although the real specimen shows an average isotropic fiber distribution, color clusters are clearly visible corresponding to the geometry and original orientation of the chopped SMC rovings. The simulation also treats the fiber orientation elementwise without coupling any elements. For a tool gap of 3 mm, the simulation shows a

clear reorientation of the fibers following the flow directions. This behavior corresponds to the experimental results. Since the material is able to flow in all in-plane directions, a typical cross shape is exhibited corresponding to the correct evolution in fiber orientation. The transition zones are also well represented. In summary, the macroscopic model tends to predict fiber alignment well. However, the geometry of the chopped rovings and the resulting increased fiber/fiber interactions are not taken into account, which can be several times larger than the required element size leading to an overestimation of the fiber orientation. Future developments must take into account the aspect of increased fiber interaction caused by the roving geometry and the high fiber content.

5 Summary

This paper shows a macroscale modeling strategy to represent the complex material behavior of SMC materials. An LS-DYNA® user-defined material model based on a building block approach for SMC materials is shown. The behavior of SMC during a compression molding process is characterized by a complex combination of mechanical, thermal and chemical effects that depends on local fiber orientation. Each individual effect is described by one individual building block that communicates by input and output parameters with neighboring building blocks. As an example, the implementation of a macroscopic fiber orientation model based on the Folgar-Tucker equation is shown. The output of the resulting fiber orientation information is realized via history variables in LS-PrePost®. For subsequent processes and analyses, it is important to include further processing possibilities for the generated usermat data. In our case, post-processing is used to prepare the data for comparison with an experimental fiber orientation measurement technique. Using the output capabilities in LS-PrePost® and a python script, the tensor information is visualized as ellipsoids and converted into planar fiber orientation angles. The following direct comparison with the experimental data shows a good tendency in predicting the fiber orientation distribution. The weaknesses of the current model were also identified and will be considered in the further developments of the material model.

6 Acknowledgement

This project is supported by the Fraunhofer ITWM and has been carried out within the framework of the “High Performance Center Simulation and Software Based Innovation”, Kaiserslautern.

7 Literature

[1] M. Neitzel, P. Mitschang, and U. Breuer: “Handbuch Verbundwerkstoffe,” 2014.

[2] V. Romanenko, M. Duhovic, D. Schommer, J. Hausmann, and J. Eschl: “Advanced process simulation of compression molded carbon fiber sheet molding compound (C-SMC) parts in automotive series applications,” *Compos Part A Appl Sci Manuf*, vol. 157, p. 106924, Jun. 2022, doi: 10.1016/j.compositesa.2022.106924.

[3] F. Gortner, A. Schüffler, J. Fischer-Schuch, and P. Mitschang: “Use of bio-based and renewable materials for sheet molding compounds (SMC) – Mechanical properties and susceptibility to fungal decay,” *Composites Part C: Open Access*, vol. 7, p. 100242, Mar. 2022, doi: 10.1016/j.jcomc.2022.100242.

[4] *Handbuch Faserverbundkunststoffe/Composites*. Wiesbaden: Springer Fachmedien Wiesbaden, 2013. doi: 10.1007/978-3-658-02755-1.

[5] C. Cherif, Ed.: *Textile Werkstoffe für den Leichtbau*. Berlin, Heidelberg: Springer Berlin Heidelberg, 2011. doi: 10.1007/978-3-642-17992-1.

[6] R. J. Silva-Nieto, B. C. Fisher, and A. W. Birley: “Rheological characterization of unsaturated polyester resin sheet molding compound,” *Polym Eng Sci*, vol. 21, no. 8, pp. 499–506, Jun. 1981, doi: 10.1002/pen.760210810.

[7] L. M. Abrams and J. M. Castro: “Predicting molding forces during sheet molding compound (SMC) compression molding. I: Model development,” *Polym Compos*, vol. 24, no. 3, pp. 291–303, Jun. 2003, doi: 10.1002/pc.10029.

[8] M. Rabinovich, K. L. Olsavsky, B. (Bud) Leach, M. Cabrera-Ríos, and J. M. Castro: “Sheet molding compound characterization using spiral flow,” *J Appl Polym Sci*, vol. 109, no. 4, pp. 2465–2471, Aug. 2008, doi: 10.1002/app.25160.

[9] M. R. Barone and D. A. Caulk: “Kinematics of flow in sheet molding compounds,” *Polym Compos*, vol. 6, no. 2, pp. 105–109, 1985, doi: 10.1002/pc.750060208.

[10] V. Romanenko: “Materialcharakterisierung und durchgängige 3D-Prozesssimulation für kohlenstofffaserverstärktes Sheet Molding Compound,” Dissertation, TU Kaiserslautern, Kaiserslautern, 2020.

[11] N. A.: “LS-DYNA® Keyword User’s Manual Volume II Material Models, LS-DYNA R12,” 2020. [Online]. Available: www.lstc.com

[12] N. A.: “LS-DYNA® Keyword User’s Manual Volume I, LS-DYNA R12,” 2020. [Online]. Available: www.lstc.com
[13] S. Hayashi, H. Chen, and W. Hu: “Compression Molding Analysis of Long Fiber Reinforced Plastics using Coupled Method of Beam and 3D Adaptive EFG in LS-DYNA ®,” in *11th European LS-DYNA® Users Conference*, Salzburg, 2017.
[14] S. Hayashi, S. Dougherty, S. Hiroi, and Y. Atsushi: “Compression Molding-Introducing New Simulation System for FRP Composites,” in *6th International LS-DYNA® Users Conference*, 2020.
[15] S. Hayashi, C. T. Wu, W. Hu, Y. Wu, X. Pan, and H. Chen: “New Methods for Compression Molding Simulation and Component Strength Validation for Long Carbon Fiber Reinforced Thermoplastics,” in *12th European LS-DYNA® Users Conference*, Koblenz, 2019.
[16] J. Teuwsen, S. K. Hohn, and T. A. Osswald: “Direct fiber simulation of a compression molded ribbed structure made of a sheet molding compound with randomly oriented carbon/epoxy prepreg strands—a comparison of predicted fiber orientations with computed tomography analyses,” *Journal of Composites Science*, vol. 4, no. 4, 2020, doi: 10.3390/jcs4040164.
[17] N. Meyer, L. Schöttl, L. Bretz, A. N. Hrymak, and L. Kärger: “Direct Bundle Simulation approach for the compression molding process of Sheet Molding Compound,” *Compos Part A Appl Sci Manuf*, vol. 132, May 2020, doi: 10.1016/j.compositesa.2020.105809.
[18] F. Folgar and C. L. Tucker III: “Orientation Behavior of Fibers in Concentrated Suspensions,” *Journal of Reinforced Plastics and Composites*, vol. 3, pp. 98–119, 1984.
[19] S. G. Advani and C. L. Tucker III: “A numerical simulation of short fiber orientation in compression molding,” *Polym Compos*, vol. 11, no. 3, pp. 164–173, 1990, doi: 10.1002/pc.750110305.
[20] C. L. Tucker III: *Fundamentals of Fiber Orientation: Description, Measurement and Prediction*. Hanser Publications, 2022.
[21] D. L. Koch: “A model for orientational diffusion in fiber suspensions,” *Physics of Fluids*, vol. 7, no. 8, pp. 2086–2088, Aug. 1995, doi: 10.1063/1.868455.
[22] H. M. Huynh: “Improved Fiber Orientation Predictions for Injection-Molded Composites,” University of Illinois at Urbana-Champaign, 2001.
[23] J. Wang, J. F. O’Gara, and C. L. Tucker III: “An objective model for slow orientation kinetics in concentrated fiber suspensions: Theory and rheological evidence,” *J Rheol (N Y N Y)*, vol. 52, no. 5, pp. 1179–1200, Sep. 2008, doi: 10.1122/1.2946437.
[24] J. H. Phelps and C. L. Tucker III: “An anisotropic rotary diffusion model for fiber orientation in short- and long-fiber thermoplastics,” *J Nonnewton Fluid Mech*, vol. 156, no. 3, pp. 165–176, Feb. 2009, doi: 10.1016/j.jnnfm.2008.08.002.
[25] A. Latz, U. Strautins, and D. Niedziela: “Comparative numerical study of two concentrated fiber suspension models,” *J Nonnewton Fluid Mech*, vol. 165, no. 13–14, pp. 764–781, Jul. 2010, doi: 10.1016/j.jnnfm.2010.04.001.
[26] H.-C. Tseng, Y.-J. Chang, T.-C. Wang, C.-H. Hsu, and R.-Y. Chang: “Three dimensional predictions of fiber orientation for injection molding of long fiber reinforced thermoplastics,” in *SPE ACCE Conference*, 2013. [Online]. Available: https://www.researchgate.net/publication/293123994
[27] H. C. Tseng and T. H. Su: “Coupled flow and fiber orientation analysis for 3D injection molding simulations of fiber composites,” in *AIP Conference Proceedings*, American Institute of Physics Inc., Feb. 2019. doi: 10.1063/1.5088279.
[28] A. Bakharev, H. Yu, S. Ray, R. Speight, and J. Wang: “Using new anisotropic rotational diffusion model to improve prediction of short fibers in thermoplastic injection molding,” in *SPE ANTEC Conference, Technical Papers*, Orlando, May 2018, pp. 7–19.
[29] J. Ernst, S. Junger, and W. Tschekalinskij: “Messung einer Faserrichtung eines Kohlefaserwerkstoffes und Herstellung eines Objekts in Kohlenstofffaserverbundbauweise,” Germany Patent DE 10 2012 220 923 A1, May 15, 2014
[30] J. Ernst, S. Junger, and W. Tschekalinskij: “Measurement of a fiber direction of a carbon fiber material and fabrication of an object in carbon fiber composite technique,” United States Patent US 9234836 B2, Jan. 12, 2016
[31] D. Schommer *et al.*: “Polarization imaging for surface fiber orientation measurements of carbon fiber sheet molding compounds,” *Composites Communications*, p. 101456, Dec. 2022, doi: 10.1016/j.coco.2022.101456.
[32] C. Diez: “qd-Build your own LS-DYNA ® Tools Quickly in Python,” in *5th International LS-DYNA® Users Conference*, 2018.